Dalton Transactions

ROYAL SOCIETY OF CHEMISTRY

PAPER

View Article Online
View Journal

Cite this: DOI: 10.1039/d5dt01479d

Data-driven prediction of HSQ polymer structure and silicon nanocrystal photoluminescence

Maharram Jabrayilov, [a] Jeremy B. Essner, [a] Abhijit Bera, [a] Vinny Paris[b,c] and Matthew G. Panthani *[a]

The synthesis of silicon nanocrystals through high-temperature pyrolysis of hydrogen silsesquioxane has emerged as a valuable approach for obtaining quantum-sized crystallites with controllable sizes and distinct photoluminescent maxima. Nevertheless, the use of commercial hydrogen silsesquioxane has notable disadvantages, such as poor shelf life, high cost, and limited supply, that motivate the exploration of alternative precursors. Recent studies have demonstrated silsesquioxane-like polymer precursors derived from molecular polysilanes (*e.g.*, trichlorosilane, triethoxysilane) that offer a cost-effective and tunable precursor for synthesizing silicon nanocrystal. Here, we elucidate the relationship between the silsesquioxane precursor chemistry, its structure, and the photoluminescence of alkyl-passivated silicon nanocrystals derived from this precursor using a statistical design of experiments technique called response surface methodology. Using this technique, we quantitatively model the relationship between precursor molar ratios, polymer structure (cage *vs.* network content), and photoluminescence quantum yield of alkyl-passivated silicon nanocrystals. We find that synthesis approaches to silsesquioxane polymers that use higher proportions of methanol and water in a trichlorosilane : water : methanol mixture result in larger amounts of network-type polymer structures, and that the network-type polymeric precursors yield silicon nanocrystals with higher photoluminescence quantum yields. While polymer structure strongly correlates with precursor composition, it is only weakly coorelated to the photoluminescence quantum yield of the resultingsilicon nanocrystals. These finding suggest factors other than precursor structure play significant roles in the photoluminescence of silicon nanocrystals.

Received 23rd June 2025,
Accepted 28th July 2025

DOI: 10.1039/d5dt01479d

rsc.li/dalton

Introduction

Silicon (Si) has long served as the foundational material in the semiconductor industry due to its favorable physical and electronic properties. Compared to other semiconductors, Si has several notable advantages: terrestrial abundance, compatibility with complementary metal–oxide–semiconductor technology, and no known intrinsic toxicity. However, Si's indirect band gap is the key, fundamental challenge for the application of next-generation computing technologies that utilize integrated photonics.[1–3] Silicon nanocrystals (SiNCs) have emerged as a potential solution due to intense, tunablephotoluminescence that arises from quantum confinement effects.[4–7] The unique photophysical properties exhibited by SiNCs, coupled with Si's aforementioned advantages, make SiNCs more appealing for many applications compared to alternatives such as III–V and II–VI quantum dots.[8,9]

A common synthetic route for SiNCs is the pyrolysis of commercially available hydrogen silsesquioxane (HSQ, FOx series, Dow Corning) in a reducing environment, yielding size-tunable (3–90 nm) SiNCs with hydride termination.[10–12] HSQ ($H_8Si_8O_{12}$) is a commonly used material in electron beam lithography because of its compact molecular structure, excellent e-beam resist roughness, and robust etching resistance.[13] Additionally, HSQ can be deposited on substrates *via* spin coating, as it is soluble in organic solvents.[14] Upon annealing at temperatures ranging from 1000 to 1400 °C, HSQ decomposes and yields a tan powder comprised of nanocrystalline silicon embedded within a silica (SiO_2) matrix. To liberate the nanocrystalline silicon and remove surface oxide species, the silica matrix is (typically) etched with hydrofluoric (HF) acid, resulting in freestanding hydride-terminated SiNCs. Several synthetic parameters have been reported to control the size and crystallinity of the hydride-terminated SiNCs, including pyrolysis temperature, pyrolysis time, and HF etch duration.[15] The surface chemistry of hydride-terminated nanocrystals can be further modified through surface reactions (such as hydrosilylation) to passivate surfaces and render them colloidally stable,

[a]Department of Chemical and Biological Engineering, Iowa State University, Ames, Iowa 50011, USA. E-mail: panthani@iastate.edu
[b]Department of Statistics, Iowa State University, Ames, Iowa 50011, USA
[c]Department of Statistics, Grinnell College, Grinnell, Iowa 50112, USA

resulting in SiNC dispersions with photoluminescence quantum yields (PLQYs) of up to 80%.[12,16–19]

Silsesquioxane polymers, denoted as $(RSiO_{1.5})_n$, where R represents H, alkyl, or aryl, have recently been investigated as alternative precursors for the synthesis of SiNCs.[19–24] These polymers have typically been synthesized through a vigorous reaction of silane precursors (such as trichlorosilane and triethoxysilane) and water/organic solvent mixtures. Depending on the reaction conditions and degree of condensation, the resulting products can either be well-defined silsesquioxane cages with varying oligomeric structures (*e.g.*, $H_8Si_8O_{12}$)[25,26] or cross-linked amorphous polymeric structures $(RSiO_{1.5})_n$ in which "cage"-type units are covalently linked with extended "network"-like structures.[19,23,24,27] These previous literature reports suggest that hydrolysis and condensation of silane precursors are highly complex processes and are impacted by many parameters such as monomer type, solvent polarity, pH, the presence of catalyst, and reaction temperature/duration. Thus, understanding the impact of these parameters is critical for controlling the resulting product's composition and morphology. Further, previous reports showed that these factors influence the size and PLQY of SiNCs.[19,20,23,28] These studies investigated the mechanism of hydrolysis–condensation reactions for synthesizing HSQ polymers from various precursors and explored the impact of cross-linking density and the ratio of "cage-" and "network-" type structures in the HSQ polymer on the resulting crystallinity, size, and optical properties of SiNCs. Nonetheless, drawing conclusions from the existing research is challenging, largely due to the fact that previous works relied on a laborious "trial and error" approach because of the large parameter space that influences the structure of silsesquioxane polymers and, consequently, the morphology and quality of SiNCs.

In this study, we explore the influence of precursor chemistry on the structure of silsesquioxane polymers synthesized from trichlorosilane and the PLQY of alkyl-stabilized SiNCs derived from the synthesized silsesquioxane polymers (Scheme 1). We employ response surface methodology (RSM), a statistical technique, to assess the impact of multiple independent variables on a given output variable.[29] The goal is to evaluate the independent continuous variables simultaneously to develop a predictive model for HSQ polymer structure. We

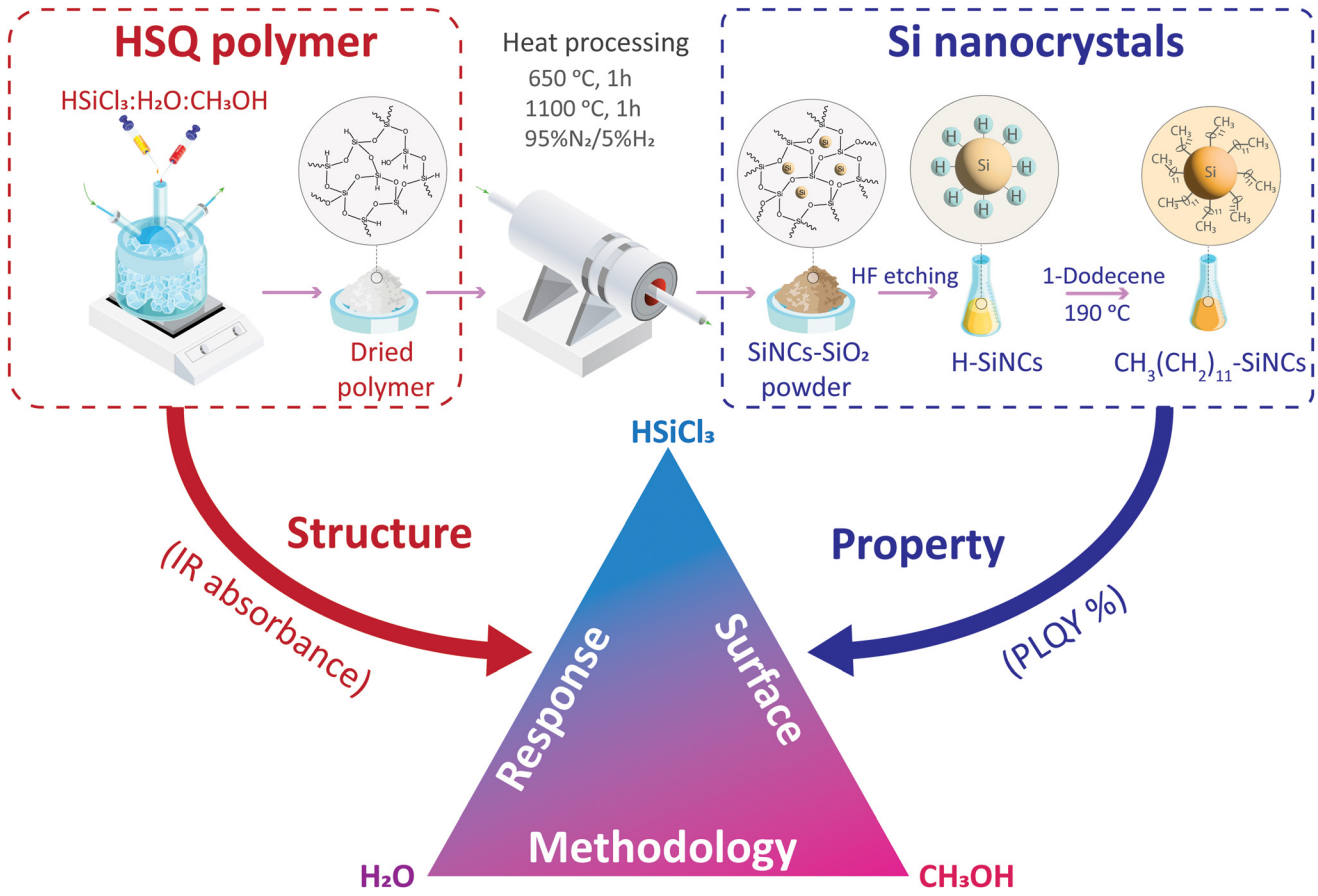

Scheme 1 Schematic summary of the study, illustrating the synthesis process of silsesquioxane-based polymers from trichlorosilane, water, and methanol, followed by the preparation of hydride (H)- and dodecyl $(CH_3(CH_2)_{11})$-terminated SiNCs. The molar ratios of trichlorosilane, water, and methanol were systematically varied. Cage content (determined by FTIR absorbance analysis) and relative photoluminescence quantum yield of SiNCs were quantified and used as response variables in Scheffé's polynomial model to predict the influence that synthetic conditions have on structural properties (cage %) of the HSQ polymer and the optical properties (PLQY %) of the resulting SiNCs.

used FTIR absorption spectra data to quantify the ratio of "cage-" and "network-" type structures in the HSQ polymer (cage : network ratios)[23] and applied Scheffé's mixed polynomial model to establish the relationship between the precursor composition (trichlorosilane : water : methanol ratio) and the resulting structure of the silsesquioxane polymers. We found that the cage : network ratio decreases with increasing water and methanol content in the reaction mixture.

We then processed these polymers at 1100 °C under forming gas (95%/5% N_2/H_2) to obtain SiNCs and subsequently alkyl passivated the NC surface through thermal hydrosilylation with 1-dodecene (Scheme 1). XRD analysis revealed that polymer precursors made without adding methanol yielded larger nanocrystals whereas the addition of both water and methanol resulted in smaller sizes. The PL peak maxima and PLQY values of alkyl-stabilized SiNCs ranged from 636 nm to 689 nm and approximately 3 to 10%, respectively. RSM modeling of the PLQY values indicated that higher PLQY was associated with lower cage : network ratios; however, the correlation is weaker than that observed between precursor ratios and polymer structure.

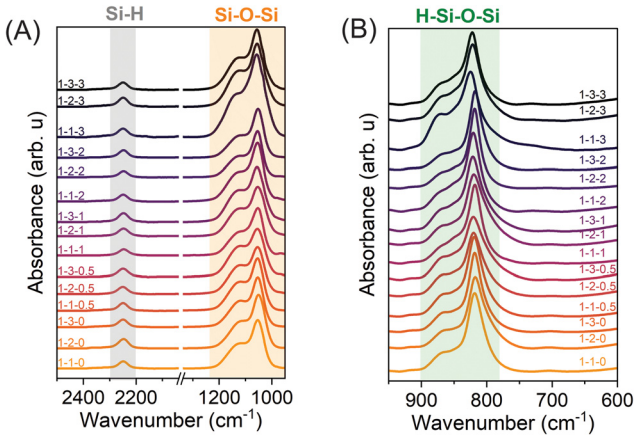

Fig. 1 FTIR spectra of the 15 silsesquioxane polymers synthesized in this work. (A) FTIR spectra plotted from 2500 to 950 cm^{-1}, highlighting Si–H and asymmetric Si–O–Si stretching vibrations. (B) FTIR spectra plotted from 950 to 600 cm^{-1}, showing H–Si–O bending and symmetric Si–O–Si vibrations. We note that molar ratios of trichlorosilane : water : methanol are denoted as 1–X_2–X_3, where X_2 and X_3 represent the molar equivalents of water and methanol, respectively. For instance, 1–1–0 corresponds to a 1 : 1 : 0 molar ratio of trichlorosilane : water : methanol.

Results and discussion

Synthesis and structural characterization of polymer precursors

First, we synthesized 15 silsesquioxane polymer precursors by modifying previously reported synthesis protocols.[20,23,30] To understand the impact of water and methanol on the structure of polymers, we varied the water : methanol molar ratios while maintaining a constant trichlorosilane molar ratio (Table S1). A full description of the experimental details is provided in the SI. Briefly, the synthesis procedure involved the rapid addition of methanol to trichlorosilane, followed by the immediate injection of water to initiate hydrolysis and condensation. For example, in the synthesis with a trichlorosilane : water : methanol molar ratio of 1 : 3 : 3, 30 mL of trichlorosilane was reacted with 41 mL of methanol and 16 mL of water. All steps were carried out under an inert argon atmosphere to prevent oxidation or side reactions.

We employed FTIR spectroscopy to understand the chemical bonding in the dried polymer precursors (Fig. 1A). All synthesized polymers have three main absorption bands: (i) a bimodal absorption band between 900 and 750 cm^{-1}, which is assigned to H–Si–O bending and symmetric Si–O–Si stretching, (ii) a second bimodal band spanning roughly from 1250 to 950 cm^{-1}, attributable to the Si–O–Si asymmetric stretching mode for cage- and network-type structures, and (iii) a band at 2250 cm^{-1} due to Si–H stretching. The observed features agree well with previously reported FTIR spectra of $(HSiO_{1.5})_n$ polymers.[19,24,31] The Si–O–Si symmetric vibration peak (~818 cm^{-1}) shifted to a slightly higher wavenumber (~824 cm^{-1}) and broadened for the three samples that were synthesized with the largest amounts of methanol (*i.e.*, 1-1-3, 1-2-3, 1-3-3). We attribute this shift to the formation of network-type structures with slightly different Si–O–Si angles.[24,32] For all polymers, Si–CH_3 stretching vibrations (~1274 cm^{-1}) were not observed, indicating that they do not contain measurable quantities of unreacted –CH_3 groups.

We integrated the FTIR absorption bands for the Si–O–Si (1250 to 950 cm^{-1}) and Si–H (2310 to 2200 cm^{-1}) features and assessed the ratio of these areas (Si–O–Si : Si–H; Fig. S1) to compare their relative quantities. We found that the Si–O–Si : Si–H ratio increased with an increasing water : methanol ratio. We attribute this trend to a decrease in the cage : network ratios. We focused more closely on the Si–O–Si peak to quantify the cage and network percentages by deconvoluting the band into Gaussian peaks (Fig. S2). Table S2 shows the deconvoluted peak maxima and the relative percentages of cage and network structures, determined from the areas under the fitted Gaussian peaks. We found that silsesquioxane polymers prepared with a trichlorosilane/water mixture (*i.e.*, without methanol) yielded higher cage : network ratios, whereas using trichlorosilane, water, and methanol resulted in lower cage : network ratios. These results suggest that polymerization of trichlorosilane using water favors cage-type structures, whereas increasing the amounts of methanol promotes the formation of higher quantities of network-type structures.

Response surface analysis of synthesis parameters and polymer structure

We applied RSM to identify the relationship between precursor ratios and the relative quantities of cage and network structures in our silsesquioxane polymer samples. The experimental design points were mapped on a ternary plot, shown in Fig. S3. For the sake of simplicity, the molar ratios of the components in the mixture were coded as a sum between 0 and 1,

listed in Table S3. Therefore, the amount of each independent variable varies from 0 to 1. We fitted Scheffé's polynomial to the data where the percentage of cage-type structures was used as the response variable and the molar ratios of trichlorosilane, water, and methanol were selected as independent variables; Scheffé's polynomial was chosen to model the data because the values of the components have a linear relationship and exist on a simplex.[33] The corners of the ternary plot are excluded from analysis, as a minimum quantity of each component is required to form a polymer product. Using the designed experimental data, we obtained a first-degree polynomial model that predicts the percentage of cage-type structure in the polymer (eqn (1)):

$$\hat{Y} = 64.62X_1 + 48.88X_2 + 42.04X_3 \quad (1)$$

where $\hat{Y}$ is the response variable (percentage of cage-type) and X_1, X_2, and X_3 are the molar fractions of trichlorosilane, water, and methanol, respectively.

The significance of each model term was evaluated using its *F*-value and associated *p*-value. Terms with *p*-values less than 0.05 were considered statistically significant, indicating a meaningful contribution to the response, while those with *p*-values greater than 0.05 were deemed insignificant. For the response variable (cage %), the model terms X_1(trichlorosilane), X_2(water), and X_3(methanol) were found to be statistically significant, with *F*-values of 1086.17, 57.72, and 48.86, respectively (Table S4). These results indicate that all three precursor components significantly influence the cage percentage. Furthermore, we found that a linear model results in an R^2 value of 0.99. Residual plots indicate no violation of the linear model assumptions (Fig. S4), demonstrating a reasonable fit with the first-degree polynomial model. The addition of second- and third-order interaction terms (trichlorosilane : water, trichlorosilane : methanol, and trichlorosilane : water : methanol) was statistically evaluated using ANOVA (Table S5). While the main effects of all three precursors were highly significant, the interaction terms were not (p = 0.23, 0.59, and 0.85 for trichlorosilane : water, trichlorosilane : methanol and trichlorosilane : water : methanol, respectively). Therefore, we opted for a main-effects model and excluded higher-order interactions.

Fig. 2 presents the predicted percentages of cage-type structures obtained from eqn (1). The plot shows that higher concentrations of trichlorosilane (relative to methanol and water) tend to increase the cage-to-network ratio, while lower concentrations result in lower cage-to-network ratios.

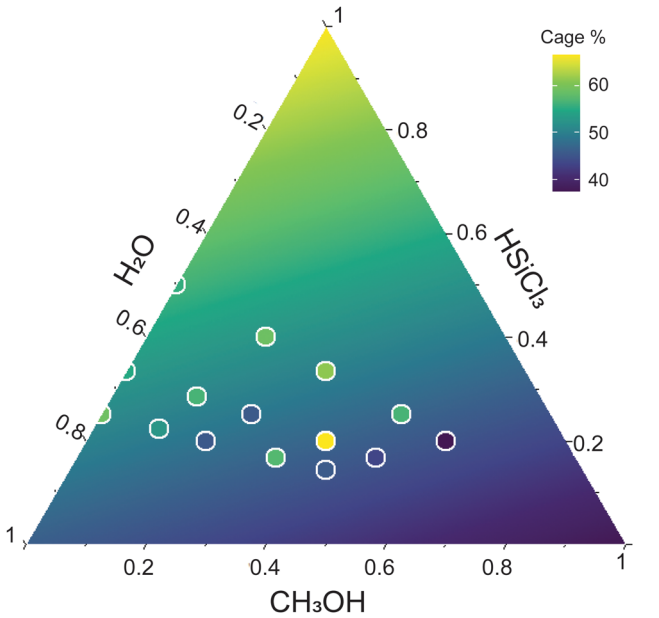

Fig. 2 Prediction of HSQ polymer structural composition with RSM using precursor molar ratios as input variables. The colored circles represent the experimental data used to fit Scheffé's polynomial model.

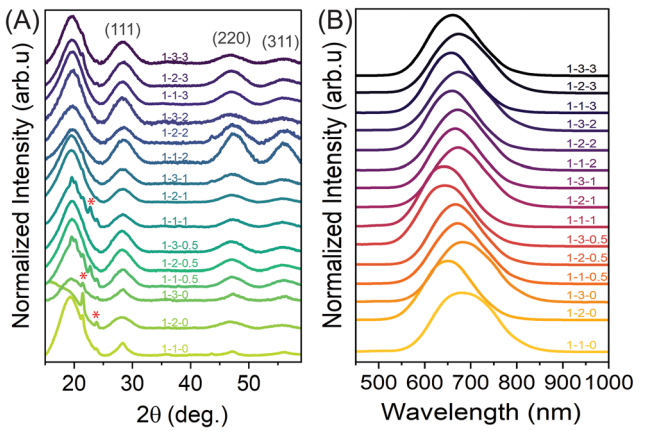

Fig. 3 Structural and optical properties of alkyl-stabilized SiNCs synthesized from different polymer precursors. (A) XRD patterns of alkyl-passivated SiNCs. Red asterisks at ~21.5°, 22.6° and 23.8° are attributed to crystalline SiO_2. (B) Photoluminescence spectra of alkyl-passivated SiNCs dispersed in toluene and excited at 385 nm. We note that molar ratios of trichlorosilane : water : methanol are denoted as $1–X_2–X_3$, where X_2 and X_3 represent the molar equivalents of water and methanol, respectively.

Optical properties of alkyl-stabilized SiNCs from silsesquioxane polymers

The polymers were thermally processed and the resulting silica powders were HF etched to liberate hydride-terminated SiNCs. Next, we thermally hydrosilylated the hydride-terminated SiNCs with 1-dodecene at 190 °C overnight under an Ar atmosphere to obtain dodecyl-passivated SiNCs. XRD (Fig. 3A) of the dodecyl-passivated NCs shows a broad reflection at 2θ of approximately 19.5°, which we attribute to residual amorphous SiO_2 resulting from poor etching, while sharper peaks (red asterisks) at 21.5°, 22.6° and 23.8° correspond to crystalline SiO_2.[34,35] For the 1 : 2 : 0 sample, a broad shoulder observed at roughly 15° is likely due to impurities introduced during the etching or sample preparation. The peaks at roughly 28.4°, 47.2° and 56.2° correspond to the (111), (220) and (311) planes for diamond cubic Si, respectively.[36] The average diameters of the NCs were determined by Scherrer analysis and are listed in

Table 1 PL properties and XRD crystallite sizes of alkyl-stabilized SiNCs

Sample mole ratios ($HSiCl_3$–H_2O–CH_3OH)	PL peak maximum (nm), λ_{ex} = 385 nm	FWHM (nm)	Crystallite size from XRD (nm)	PLQY (%), λ_{ex} = 421 nm
1–1–0	688	147	4	4.3
1–2–0	652	125	2.1	4.1
1–3–0	689	143	3.5	5.5
1–1–0.5	675	131	2.2	7.8
1–2–0.5	670	123	2.1	3.5
1–3–0.5	647	129	2.2	9.5
1–1–1	645	119	2.4	8.8
1–2–1	676	133	2.3	4.3
1–3–1	669	122	2.2	6
1–1–2	675	131	2.2	5.9
1–2–2	661	122	2.2	5.2
1–3–2	679	139	2	3.8
1–1–3	659	119	2.2	4.1
1–2–3	636	117	2.1	7.1
1–3–3	663	128	2	10.2

Table 1. The polymers that were synthesized with only trichlorosilane and water yielded NCs with diameters ranging between ~3.4 and 3.9 nm. In contrast, the polymer synthesis that included methanol produced smaller nanocrystals with an average diameter of approximately 2 to 2.1 nm. The decrease in size is attributed to the lower cage : network ratio in the polymer precursor; we propose that the predominant network-like structure impedes diffusion of silicon atoms during thermal processing, resulting in smaller-sized nanocrystals.

We characterized the photoluminescence (PL) of the alkyl-stabilized SiNCs at room temperature, employing a 385 nm LED as the excitation source (Fig. 3B). The PL peak maxima and full-width at half-maximum (FWHM) values ranged from roughly 636 nm to 689 nm and 117 to 147 nm, respectively (Table 1). The trends show that there is a correlation between the PL peak maxima and FWHM; as the PL peak maximum decreases, the FWHM gets narrower. We attribute the peak narrowing to a decrease in the distribution of emissive states, arising from more homogeneous size distribution. The effect of precursor chemistry on size distribution can be rationalized by understanding the impact of the different polymer structures on the reactive processes that occur during thermal processing. Higher fractions of network-type structures are known to impede the diffusion of the Si species in the SiO_2 matrix during annealing and lead to more localized nucleation sites for SiNCs,[20] which restricts NC growth and results in smaller SiNCs with more uniform size distributions. We have not excluded the possibility that variations in the surface chemistry could also contribute to differences in PL FWHM and PLQY.[37] Poor surface passivation can introduce surface trap states, which increase non-radiative recombination and result in a broader emission band. However, this study specifically aims to isolate the effects of precursor chemistry on photoluminescence.

Next, we determined the relative PLQY values of all SiNCs using Coumarin 153 as a reference fluorophore,[38] as summarized in Table 1. We note that a 421 nm excitation source was used for the calculation of the relative PLQYs in Table 1, as the absorbance of the reference fluorophore is negligible below 400 nm. The relative PLQY values ranged from 3 to 10%, which is lower than previously reported PLQY values for SiNCs.[19,23,24] The relatively low PLQYs observed in our alkyl-stabilized SiNCs may result from insufficient surface passivation by thermal hydrosilylation, which typically yields lower surface coverage compared to radical-initiated passivation[39] and introduces non-radiative trap states.

Relationship between polymer structure and PLQY

We again applied RSM to gain insight into the relationship between polymer structure and photoluminescence, using PLQY as a response variable. The first-degree polynomial model for the prediction of the percentage of PLQY was determined (eqn (2)):

$$\hat{Y} = 3.91X_1 + 6.34X_2 + 7.43X_3 \quad (2)$$

ANOVA results indicate that all three precursor components —trichlorosilane, water, and methanol—have a statistically significant influence on the PLQY, with p-values of 8.816×10^{-7}, 0.0276, and 0.0101, respectively (Table S6). Trichlorosilane exhibited the strongest effect, as reflected by its low p-value and high F-value of 84.5. Similar to the case of cage percentages of the HSQ polymer, the interaction terms (trichlorosilane : water, trichlorosilane : methanol, and trichlorosilane : water : methanol) were not statistically significant ($p > 0.05$), indicating that interaction effects among the precursors do not meaningfully contribute to the variation in PLQY (Table S7). The linear model was fit with an R^2 value (0.89) (see Fig. S5 for residuals), which indicates that the correlation between precursor ratios and PLQY of SiNCs is weak compared to the correlation between precursor ratios and the resulting HSQ polymer structure. Fig. 4 demonstrates a contour plot of predicted PLQY values obtained with eqn (2). Our predicted model suggests that PLQY values are higher near the right corner of the triangle in which polymers are obtained with a higher concentration of methanol. Based on our previous conclusion for the structure of polymers, near the right corner of the triangle, silsesquioxane polymers have lower cage : network ratios, implying that a greater network-like content in the polymer precursor results in higher PLQY. We also note that our results differ from the conclusions recently drawn by the Saitow group,[19,23] who demonstrated that higher proportions of cage-type structures in the polymer precursor correlate with increased PLQY values. However, we note that the PLQY of NCs can also be impacted by other factors that are not being considered, such as the degree of surface passivation with ligands, the choice of solvent for QY measurements, and the purification of nanocrystals. This points towards F3 a need for future work that accounts for other experimental parameters to more accurately understand the factors that impact PLQY.

Verification of Scheffé's polynomial models

To evaluate the predictive capability of our statistical model, we synthesized six new samples with either higher quantities

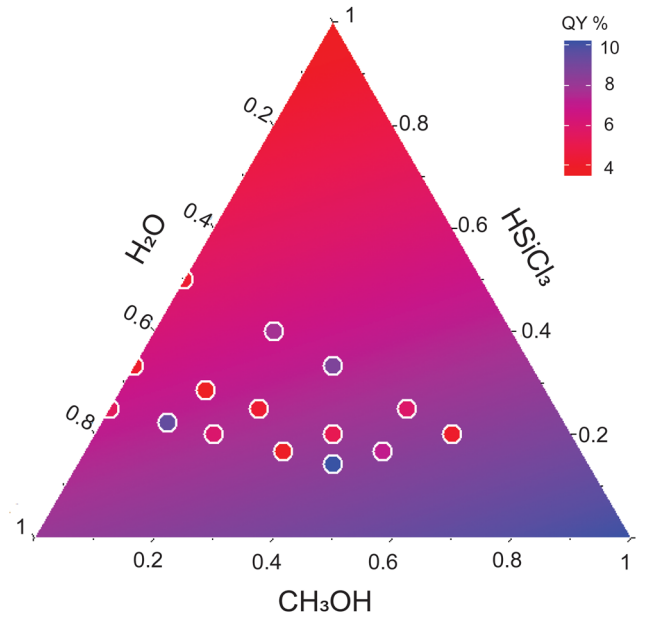

Fig. 4 Prediction of PLQY (%) values of alkyl-stabilized SiNCs with RSM using precursor molar ratios as input variables. The colored circles represent the experimental data used to fit Scheffé's polynomial model.

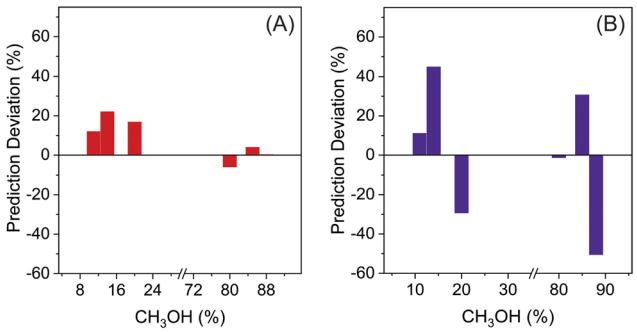

Fig. 5 Deviations between predicted and experimentally determined values for (A) cage-type structures (%) in HSQ polymers and (B) photoluminescence quantum yield (PLQY, %) of alkyl-stabilized SiNCs synthesized from selected precursor molar ratios. In both plots, the *y*-axis represents the relative deviation (Predicted − Experimental)/Predicted × 100, while the *x*-axis corresponds to the percentages of methanol in the trichlorosilane/water/methanol reaction mixture.

of methanol or water. Three of those samples were synthesized by maintaining a constant water : trichlorosilane ratio of 1 : 1 while varying methanol ratios from 4 to 8. Similarly, the remaining three samples were prepared by keeping the methanol : trichlorosilane ratio (1 : 1) constant and altering water molar ratios from 4 to 8. Polymers synthesized from these precursors (Fig. S6) have three main absorption bands in FTIR that are associated with H–Si, Si–O–Si, and H–Si–O vibrations. The deconvolution of the Si–O–Si stretching band reveals the formation of higher network-type structures in nearly all samples, with the exception of those synthesized using a 1 : 1 : 4 trichlorosilane : water : methanol ratio (Fig. S7). Fig. 5A shows the deviations between the predicted and experimentally determined cage-type structure percentages. Under conditions of higher water concentrations, the model overestimated the cage content by approximately 17% on average. In contrast, samples synthesized with higher methanol amounts in the reaction mixture exhibited minimal deviations, ranging from 0.44% to 6%. These supplementary experimental results reinforce the predictive accuracy of our RSM model across a wide range of precursor ratios, supporting its robustness in predicting the structural contents of HSQ polymers.

Next, we examined the photoluminescence properties of alkyl-stabilized SiNCs derived from polymers synthesized by using selected molar ratio points. As shown in Fig. S8A, the XRD patterns of the resulting SiNCs are consistent with the patterns of the samples used to generate the model, as well as previously reported diffraction patterns, confirming the crystalline nature of the materials. The corresponding photoluminescence (PL) spectra of alkyl-stabilized SiNCs are presented in Fig. S8B. We note that samples 1–1–8, 1–4–1, and 1–8–1 exhibit PL spectra with non-Gaussian profiles. These deviations likely originate from a combination of broader size distributions and surface-related effects. In particular, incomplete surface passivation may introduce multiple emissive states that distort or broaden the emission features, while variations in nanocrystal size can lead to a heterogeneous distribution of bandgap energies, resulting in asymmetric or broadened PL spectra. Table S8 summarizes the PL peak maxima, FWHM, and crystallite sizes. Fig. 5B shows the deviations between predicted and experimentally determined PLQY values. Conversely to the cage-type structure predictions for the polymer precursor, the predicted PLQY values of the alkyl-stabilized SiNCs were substantially overestimated by Scheffé's polynomial model. These findings indicate a weak correlation between the PLQY of the SiNCs and the amount of cage and network structures in the HSQ polymer, implying that other factors—such as the degree of surface passivation, the presence of defects on the surface, nanocrystal size distribution, or differences in the alkyl ligand coverage—may play a more critical role in determining PLQY and should be considered in future model refinements.

Conclusions

In summary, we synthesized silsesquioxane polymers using hydrolysis and condensation reactions. By controlling the precursor composition, we varied the fraction of cage- and network-type structures. We characterized the relative amounts of cage- and network-type structures using FTIR absorption spectra. We developed an RSM model that predicts the relationships between experimental synthesis parameters (molar ratios) and polymer structure. With the RSM model, we found that lower concentrations of trichlorosilane in the reaction mixture form silsesquioxane polymers with a lower cage : network ratio. Additionally, we successfully processed the polymer into alkyl-stabilized SiNCs, which had PL peak posi-

tions ranging from 636 nm to 689 nm and PLQY between 3% and 10%. The RSM analysis determined a correlation between precursor chemistry, polymer structures, and PLQY values, suggesting that silsesquioxane polymers with lower cage : network ratios yield NCs with higher PLQY; however, the lower R^2 value (0.89) for fit indicates a weak correlation between the PLQY of the SiNCs and precursor ratios. This suggests that other factors—such as surface passivation, defect density, nanocrystal size distribution, and ligand coverage—may have a stronger influence on the photoluminescence (*i.e.*, PLQY) of SiNCs. Future work should focus on investigating the influence of these additional factors on the optical properties of SiNCs, namely PLQY. A deeper understanding of these aspects will be crucial for the development of high-quality SiNCs with enhanced optical properties, which are essential for applications in next-generation nanoscale optoelectronic devices.

Author contributions

Maharram Jabrayilov: conceptualization, methodology, investigation, validation, data curation, formal analysis, visualization, and writing – initial draft, review, and editing; Jeremy B. Essner: investigation, data curation, and writing – review and editing; Abhijit Bera: investigation, data curation, and writing – review and editing; Vinny Paris: investigation, data curation, and writing – review and editing; and Matthew G. Panthani: funding, resources, conceptualization, project administration, supervision, visualization, and writing – initial draft, review, and editing.

Conflicts of interest

There are no conflicts to declare.

Data availability

Data for this article are available at Mendeley Data at DOI: **https://doi.org/10.17632/spjshrsh7f.1**.

Supplementary information is available: Experimental details, XRD, FTIR, PL, RSM analysis details. See DOI: **https://doi.org/10.1039/d5dt01479d**.

Acknowledgements

This material is based upon work supported by the National Science Foundation under Grant No. DMR-2350483, which supported material synthesis. The authors would also like to acknowledge funding from the Air Force Office of Scientific Research under Award FA9550-20-10018. Purchase of Bruker Apex II CCD Single Crystal Diffractometer used to obtain results included in this publication was supported by the National Science Foundation under Grant No. CHE 0840305. We would like to acknowledge Dr Arkady Ellern for his assistance with X-ray diffraction measurements at the ISU Chemical Instrumentation Facility. Any opinions, findings, and conclusions or recommendations expressed in this material are those of the author(s) and do not necessarily reflect the views of the National Science Foundation.

References

1 E. O. Kane, *Phys. Rev.*, 1966, **146**, 558.
2 F. Herman, *Proc. IRE*, 1955, **43**, 1703–1732.
3 A. H. Atabaki, S. Moazeni, F. Pavanello, H. Gevorgyan, J. Notaros, L. Alloatti, M. T. Wade, C. Sun, S. A. Kruger and H. Meng, *Nature*, 2018, **556**, 349–354.
4 S. Furukawa and T. Miyasato, *Jpn. J. Appl. Phys.*, 1988, **27**, L2207.
5 B. Delley and E. F. Steigmeier, *Phys. Rev. B: Condens. Matter Mater. Phys.*, 1993, **47**, 1397.
6 M. L. Brongersma, P. G. Kik, A. Polman, K. S. Min and H. A. Atwater, *Appl. Phys. Lett.*, 2000, **76**, 351–353.
7 L. T. Canham, *Appl. Phys. Lett.*, 1990, **57**, 1046–1048.
8 A. J. Nozik and O. I. Mićić, *MRS Bull.*, 1998, **23**, 24–30.
9 L. Yang, S. Zhang, B. Xu, J. Jiang, B. Cai, X. Lv, Y. Zou, Z. Fan, H. Yang and H. Zeng, *Nano Lett.*, 2023, **23**, 2443–2453.
10 C. M. Hessel, E. J. Henderson and J. G. C. Veinot, *Chem. Mater.*, 2006, **18**, 6139–6146.
11 C. M. Hessel, E. J. Henderson and J. G. C. Veinot, *J. Phys. Chem. C*, 2007, **111**, 6956–6961.
12 C. M. Hessel, D. Reid, M. G. Panthani, M. R. Rasch, B. W. Goodfellow, J. Wei, H. Fujii, V. Akhavan and B. A. Korgel, *Chem. Mater.*, 2011, **24**, 393–401.
13 H. Namatsu, Y. Takahashi, K. Yamazaki, T. Yamaguchi, M. Nagase and K. Kurihara, *J. Vac. Sci. Technol., B: Microelectron. Nanometer Struct.–Process., Meas., Phenom.*, 1998, **16**, 69–76.
14 G. M. Schmid, L. E. Carpenter and J. A. Liddle, *J. Vac. Sci. Technol., B: Microelectron. Nanometer Struct.–Process., Meas., Phenom.*, 2004, **22**, 3497–3502.
15 J. R. Rodríguez Núñez, J. A. Kelly, E. J. Henderson and J. G. C. Veinot, *Chem. Mater.*, 2012, **24**, 346–352.
16 M. Locritani, Y. Yu, G. Bergamini, M. Baroncini, J. K. Molloy, B. A. Korgel and P. Ceroni, *J. Phys. Chem. Lett.*, 2014, **5**, 3325–3329.
17 T. Ono, Y. Xu, T. Sakata and K. Saitow, *ACS Appl. Mater. Interfaces*, 2022, **14**, 1373–1388.
18 M. Amirul Islam, M. Hosnay Mobarok, R. Sinelnikov, T. K. Purkait and J. G. C. Veinot, *Langmuir*, 2017, **33**, 8766–8773.
19 H. Ueda and K. Saitow, *ACS Appl. Mater. Interfaces*, 2023, **16**, 985–997.
20 E. J. Henderson, J. A. Kelly and J. G. C. Veinot, *Chem. Mater.*, 2009, **21**, 5426–5434.
21 N. Shirahata, *Sci. Rep.*, 2022, **12**, 17211.
22 İ. Nur Gamze Özbilgin, B. Ghosh, H. Yamada and N. Shirahata, *J. Phys. Chem. C*, 2021, **125**, 3421–3431.

23 S. Terada, Y. Xin and K. Saitow, *Chem. Mater.*, 2020, **32**, 8382–8392.
24 J. Zhou, J. Huang, H. Chen, A. Samanta, J. Linnros, Z. Yang and I. Sychugov, *J. Phys. Chem. Lett.*, 2021, **12**, 8909–8916.
25 C. L. Frye and W. T. Collins, *J. Am. Chem. Soc.*, 1970, **92**, 5586–5588.
26 P. A. Agaskar, *Inorg. Chem.*, 1991, **30**, 2707–2708.
27 W. Liu, Y. Yu and W. Chen, *J. Appl. Polym. Sci.*, 2004, **91**, 2653–2660.
28 G. D. Soraru, S. Modena, P. Bettotti, G. Das, G. Mariotto and L. Pavesi, *Appl. Phys. Lett.*, 2003, **83**, 749–751.
29 R. H. Myers, D. C. Montgomery and C. M. Anderson-Cook, *Response surface methodology: process and product optimization using designed experiments*, John Wiley & Sons, 2016.
30 J. Zhou, J. Huang, H. Chen, A. Samanta, J. Linnros, Z. Yang and I. Sychugov, *J. Phys. Chem. Lett.*, 2021, **12**, 8909–8916.
31 M. J. Loboda, C. M. Grove and R. F. Schneider, *J. Electrochem. Soc.*, 1998, **145**, 2861.
32 M. J. Loboda, C. M. Grove and R. F. Schneider, *J. Electrochem. Soc.*, 1998, **145**, 2861.
33 J. A. Cornell, *Experiments with mixtures: designs, models, and the analysis of mixture data*, Wiley-interscience, 1843, vol. 255.
34 R. T. Downs and D. C. Palmer, *Am. Mineral.*, 1994, **79**, 9–14.
35 W. A. Dollase and W. H. Baur, *Am. Mineral.*, 1976, **61**, 971–978.
36 J. M. Westra, V. Vavruňková, P. Šutta, R. Van Swaaij and M. Zeman, *Energy Procedia*, 2010, **2**, 235–241.
37 K. Dohnalová, T. Gregorkiewicz and K. Kůsová, *J. Phys.: Condens. Matter*, 2014, **26**, 173201.
38 K. Rurack and M. Spieles, *Anal. Chem.*, 2011, **83**, 1232–1242.
39 R. J. Clark, M. Aghajamali, C. M. Gonzalez, L. Hadidi, M. Amirul Islam, M. Javadi, M. Hosnay Mobarok, T. K. Purkait, C. Jay, T. Robidillo, R. Sinelnikov, A. N. Thiessen, J. Washington, H. Yu and J. G. C. Veinot, *Chem. Mater.*, 2016, **29**, 80–89.